

Final Report for "Studies of MGS TES and MPF MET Data"

NASA Mars Data Analysis Program Grant NAG5-9771

Principal Investigator: Jeff R. Barnes

**Professor of Atmospheric Sciences, College of Oceanic and Atmospheric
Sciences, Oregon State University, Corvallis, OR 97331**

Brief Summary of Work

The work supported by this grant was divided into two broad areas: (1) mesoscale modeling of atmospheric circulations and analyses of Pathfinder, Viking, and other Mars data, and (2) analyses of MGS TES temperature data.

The mesoscale modeling began with the development of a suitable Mars mesoscale model based upon the terrestrial MM5 model, which was then applied to the simulation of the meteorological observations at the Pathfinder and Viking Lander 1 sites during northern summer. This extended study served a dual purpose: to validate the new mesoscale model with the best of the available in-situ data, and to use the model to aid in the interpretation of the surface meteorological data. This work resulted in a paper which has appeared in the *Journal of Geophysical Research* (Tyler et al., 2002). This paper summarizes most of this work and presents the key comparisons with the data in detail. During the last year of the project, the focus of the mesoscale circulation studies was changed to the north polar region in summertime. This region is of critical importance for the current Mars climate system, since the residual north ice cap appears to be the primary source of atmospheric water on annual time scales. The polar mesoscale studies were begun with analyses of polar TES and radio occultation data, and with the generation of suitable polar maps of thermal inertia and albedo (making use of the latest TES-derived data).

The TES temperature data analyses have made use of the Fast Fourier Synoptic Mapping (FFSM) technique to produce synoptic temperature maps from the highly asynchronous TES data. This technique

provides unique advantages relative to other possible analysis methods. At the conclusion of the grant period, a very sizeable fraction of the available (two full Mars years) TES temperature data had been at least preliminarily analyzed using the FFSM approach. Temperature maps have been produced for a sizeable fraction of the TES data set. These maps are of several types, including ones that isolate the traveling weather systems in middle and high latitudes on Mars. In addition to the temperature maps, wind maps were also generated using a linearized balance method. The combination of wind and temperature maps allows the calculation of the heat and momentum fluxes produced by the weather systems. The FFSM analyses yield space-time power spectra as an intermediate data product, and these allow some of the key properties of the Mars weather systems to be readily identified. A number of talks and extended abstracts have resulted from the FFSM studies of the TES temperature data; these are listed in the Bibliography and several are attached to this Final Report. The preparation of several papers for submission to journals is now underway.

Bibliography

2003: Planetary Eddies in the Martian Atmosphere: FFSM Analysis of TES Data, J.R. Barnes, Mars Atmosphere Modeling and Observations Workshop, Granada, Spain.

2003: Development of the OSU Mars MM5 and Description of Initial Results, D. Tyler and J.R. Barnes, Mars Atmosphere Modeling and Observations Workshop, Granada, Spain.

2003: Simulating the Late Summer Circulation of the Martian North Polar Region, D. Tyler and J.R. Barnes, Mars Atmosphere Modeling and Observations Workshop, Granada, Spain.

2003: Mars Weather Systems and Maps: FFSM Analyses of MGS TES Temperature Data, J.R. Barnes, abstract submitted for the 6th International Mars Conference, Pasadena, CA.

2003: Diurnal and Subdiurnal Variability in the Mars Pathfinder Presidential Meteorology Sessions, M.S. Thesis, Oregon State University, 246 pp. (S. Bennett)

2002: Simulation of Surface Meteorology at the Pathfinder and VL1 Sites Using a Mars Mesoscale Model, *J. Geophys. Res.*, **107**, No. E4, 2-1 – 2-20 (D. Tyler, J.R. Barnes, and R.M. Haberle).

2001: Baroclinic Eddies in the Martian Atmosphere: A General Circulation Model Study, M.S. Thesis, Oregon State University, 145 pp. (M. Matheson)

2001: Asynoptic Fourier Transform Analyses of MGS TES Data: Transient Baroclinic Eddies, J.R. Barnes, 33rd Meeting of the AAS Division for Planetary Sciences, New Orleans, LA, *Bull. Amer. Astron. Soc.*, 33, p. 1088-1089.

2000: The Current Atmospheric Circulation and Climate of Mars: The Polar Regions, J.R. Barnes, The Second International Conference on Mars Polar Science and Exploration, Reykjavik, Iceland (Invited Review Talk), LPI Contribution Number 1057, p. 5.

2000: Initial 3-D Mesoscale Simulations of the North Pole Martian Summer Atmospheric Circulation, D. Tyler and J.R. Barnes, The Second International Conference on Mars Polar Science and Exploration, Reykjavik, Iceland, LPI Contribution Number 1057, p. 178.

2000: Transient Baroclinic Eddies in the Martian Atmosphere: Seasonality and Baroclinic Sensitivity, J.R. Barnes and M. Matheson, 32nd Meeting of the AAS Division for Planetary Sciences, Pasadena, California, *Bull. Amer. Astron. Soc.*, 32, pp. 1091-1092.

SIMULATING THE LATE-SUMMER ATMOSPHERIC CIRCULATION OF THE MARTIAN NORTH POLE REGION.

D. Tyler¹ and J.R. Barnes²,

¹College of Oceanic and Atmospheric Sciences, Oregon State University, Corvallis, OR, USA, dtyler@coas.oregonstate.edu

²College of Oceanic and Atmospheric Sciences, Oregon State University, Corvallis, OR, USA, barnes@coas.oregonstate.edu

Introduction: Pictures taken from orbit over the north pole residual ice cap certainly suggest that atmospheric circulations have played an important role in the evolution of its present day appearance. One can hardly examine such images without envisioning a well-developed polar vortex. A more complete understanding of the late-summer atmospheric circulation for this region will help us understand the present day climatological stability of the residual cap. It is to this end that we begin a study of the polar circulation.

Our Model and Method: The computer model being used in this study is the Oregon State University Mars MM5 (OSU MMM5). Our model was developed by modifying the Penn State/NCAR MM5 so it could be used to simulate mesoscale circulations on Mars. For boundary and initial conditions the model uses output from the NASA Ames Mars GCM. The development of the model and the studies it has been used in are outlined in another abstract submitted for this workshop.

Methodology. Our approach to determining the circulation of the north-polar region is to first tune the model so it predicts surface and atmospheric temperatures that match data gathered during the Mars Global Surveyor (MGS) mission. With the MMM5 tuned to simulate the actual data we can then examine the simulated circulation with greater confidence in its accuracy. At this initial stage we are primarily concerned with simulating the temperature structure over the actual ice cap. Thus, the relevant data are 1) daytime and nighttime MGS/TES residual cap temperatures and 2) atmospheric temperature profiles from over the ice cap. The temperature profiles being used for this purpose are publicly available on the website of the MGS Radio Science (RS) team [1].

Tuning the MMM5 is a straightforward iterative process: 1) compare the zonal mean temperature profile of the model with that of data at 85.1° N, 2) adjust tunable parameters, 3) rerun the model and 4) compare the temperatures again. The global dust loading is a tunable parameter in both the GCM and the MMM5. In the MMM5 we additionally treat the deepest “soil” (ice) temperature as a tunable parameter. This approach was chosen because of the large subsurface heat flux values that are required in the polar heat balance during this season [2]. The deep “soil” (ice) tempera-

tures of the residual cap in the model are initialized using annual average temperatures instead of diurnal averages (the MM5 uses diurnal average surface temperature by default to initialize the deepest soil temperature). Model initialization in the MMM5 is thus modified with a logical check to reset the deep “soil” (ice) temperature if the albedo is above a critical value. We are also setting the thermal inertia to an appropriate ice value dependent upon the albedo check. Presently we are using 175 K for the deep “soil” (ice) temperature and a thermal inertia of $900 \text{ J m}^{-2} \text{ s}^{1/2} \text{ K}^{-1}$ for the ice locations.

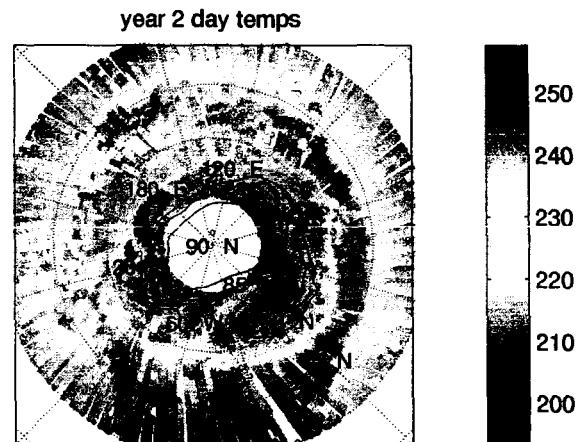


Figure 1: Daytime surface temperatures for the seasonal period ($130 < L_s < 140$). Temperature data is uniformly distributed across 1300-1400 hrs. Some contours from the MMM5 18 km nest topography are shown for reference.

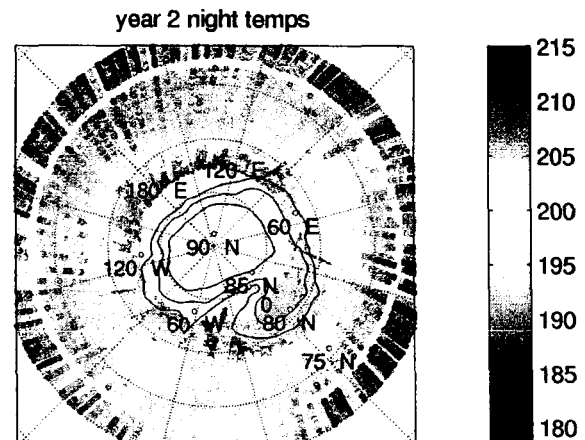


Figure 2: Nighttime surface temperatures for the seasonal period ($130 < L_s < 140$). Temperature data is uniformly distributed across 0300-0400 hrs. Some contours from the MMM5 18 km nest topography are shown for reference.

The Data: In Figs. 1 and 2 we show the respective daytime and nighttime TES surface temperatures that are being used to tune the MMM5 polar surface properties (thermal inertia and albedo). The local times of these data are approximately 1330 and 0330 hrs; the season is $130 < L_s < 140$. Daytime ice temperatures are fairly well represented in Fig. 1, but the nighttime temperature coverage in Fig. 2 is minimal.

For atmospheric temperatures we are using 99 RS profiles from this same seasonal period. These temperature profiles are tightly grouped around 85.1° N latitude. The mean time of the profiles is 0630 hrs and the L_s distribution is uniform over $130 < L_s < 140$.

Comparison With MMM5: Given the narrow latitude range of the RS temperature profiles, their uniform distribution in longitude, season and LST, it seems sufficient to use a simple average to form a zonal mean temperature profile. Locations of the RS profiles and the MMM5 data interpolations are shown in Fig. 3 over a map of the TES albedo that is presently being used in the model. The ice albedo values of this map are too low; presently we are considering ways to modify our datasets and maintain the resolution that is required to accurately resolve ice surfaces within the high-resolution topography of these simulations.

Location of "Over Ice" RS Profiles on MMM5 Albedo

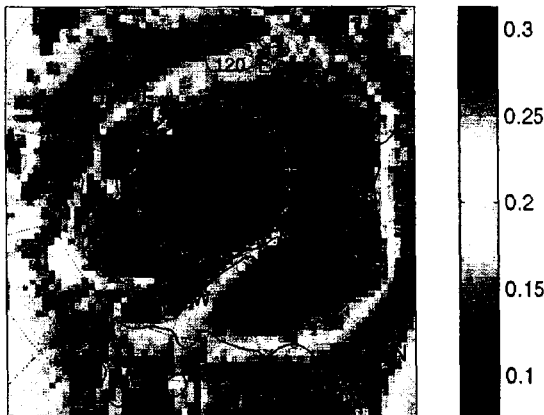


Figure 3: Locations of RS temperature profiles (black dots) and the MMM5 interpolations (cyan stars). The background map shows albedo and contours of the topography used in the 18 km polar nest.

To generate a zonal mean temperature profile for the MMM5 a simple average of model profiles was used. In Fig. 4 we show all of the RS and MMM5 profiles and the respective zonal means. The zonal means agree quite well throughout the bulk of the atmosphere

although there is a much stronger near-surface inversion in the MMM5 zonal mean than there is in the RS data mean profile. Most of this inversion is aliasing of the model mean profile due to profiles that are over non-ice locations in the model.

Forward From Here: At this point we are still working to finalize our model configuration. We especially need to modify the albedo values and it will help greatly to have thermal inertia coverage to higher latitudes than we presently have. This work will move forward and we expect to have some interesting results to present in Granada.

RS Profiles at $130 < L_s < 140$ (6:30 AM mean)

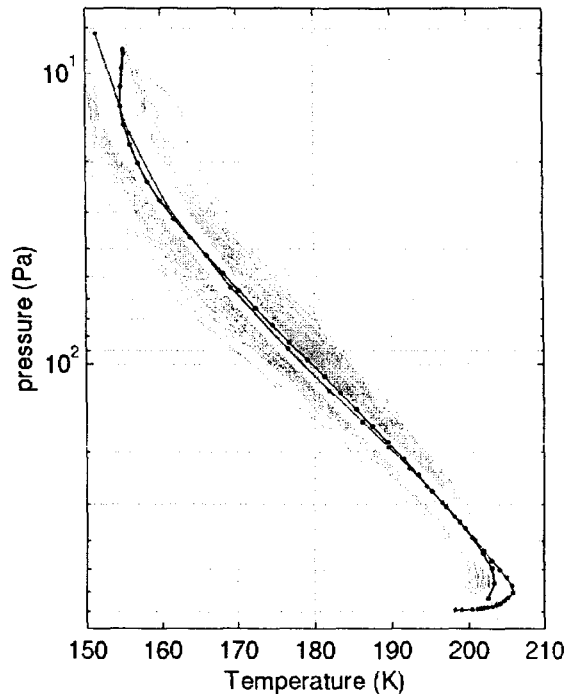


Figure 4: The 99 RS temperature profiles (cyan) and their average (black line/points) are shown along with 8 sols of MMM5 profiles (yellow) and their average (red line/points).

References:

- [1] <http://nova.stanford.edu/projects/mgs>
- [2] Paige and Ingersoll, Science, 228, 1160-1168.

Planetary Eddies in the Martian Atmosphere: FFSM Analysis of TES Data

J.R. Barnes, *College of Oceanic and Atmospheric Sciences, Oregon State U., Corvallis, OR, 97333, USA.*

Introduction:

Planetary scale eddies of various types play very important roles in the general circulation of the Martian atmosphere and in the climate system of Mars. In particular, transient baroclinic eddies (midlatitude weather systems) and quasi-stationary eddies are prominent. Both types of eddies are fundamentally analogous to their counterparts in the terrestrial atmosphere, opening up excellent opportunities for comparative studies. Transient baroclinic eddies were predicted to be present in middle and high latitudes in the fall, winter, and spring on Mars on the basis of theory and GCM simulations (1). The Viking Lander Meteorology data allowed their existence to be verified, and some of their most basic properties to be determined (2,3). Quasi-stationary eddies were also predicted by theory and modeling to be present in all seasons, in both the tropics and the extratropics. Viking IRTM data appeared to evidence these eddies, and MGS TES and RS data have recently allowed their existence to be confirmed (4).

The MGS TES data allow the determination of the basic properties and dynamics of the transient baroclinic and quasi-stationary eddies. This can be done in different ways. We have utilized a technique referred to as Fast Fourier Synoptic Mapping (FFSM), in order to do this with the TES nadir temperature data. To date we have analyzed in detail a sub-set of all of the data, focusing upon seven time intervals averaging about 40-50 sols in length.

Data Analysis:

The FFSM technique was originally developed some time ago (5,6), but it has not been used very much with terrestrial data. It offers some very considerable benefits, however. In particular, it allows the production of twice-daily synoptic maps from the highly asynchronous TES data. These maps reflect the full space-time resolution of the data, which extends to zonal wavenumber 6 and to periods slightly shorter than 1 sol (for eastward traveling waves). Relatively higher frequency (1-3 sols) features are not distorted or smoothed by the FFSM analysis, something that is often a major problem with other methods. An intermediate product of the FFSM analysis is a set of spectra for the interval being examined. These spectra allow the identification of the dominant wave modes which are present in the data, and the characterization of their amplitude and phase structures. The volume of the TES data allows the

spectra to have very high statistical significances, which allows even quite weak eddies to be found. The synoptic maps allow the full time evolution of the disturbances to be seen, and they provide a starting point for the computation of various higher-order quantities (winds, heat and momentum fluxes, EP fluxes, etc.).

The FFSM analyses require considerable pre-processing of the data. First the data must be sorted into ascending and descending orbit observations for each latitude bin and TES pressure level. We have chosen to "oversample" in the vertical (using ~ 15 levels), and to employ one degree latitude bins spaced at 5 degree intervals. The small bin size greatly helps to avoid aliasing due to very sharp meridional gradients in the data. All gaps in the data then have to be filled in using interpolation schemes – either interpolating along an orbit or interpolating between orbits for longer gaps. After close examination of the resulting time series of data, the basic FFSM analysis can be carried out for each latitude bin and vertical level. This analysis yields the twice-daily maps as well as the spectra – one for each zonal wavenumber, and for each latitude and vertical level (typically, a very large number of spectra). The maps can be produced in various ways, depending on how one selects the spectral coefficients to be used in the mapping. We have produced maps of the full temperature fields as well as maps of the transient eddy part of the temperature fields as standard products; other maps can be very useful in various circumstances. The maps can be produced at much higher time resolutions (as well as much higher longitudinal resolutions – we have used 5 degrees as a standard) than twice-daily in order to facilitate the detailed study of transient features via movies, but the true resolution of the data is equivalent to two maps per sol.

The spectra are examined closely in order to identify the dominant spectral peaks. These then lead to the selection of multiple frequency-band modes, at each zonal wavenumber. The amplitudes and phases of the wave modes are then calculated from the spectral coefficient values.

The seven data intervals which we have chosen for analysis to date include two that surround northern winter solstice during the first mapping year, one earlier in the winter (prior to the major dust storm event) of that first year, one surrounding northern spring equinox during the first mapping year, two intervals surrounding southern winter solstice in the second mapping year, and one interval during the

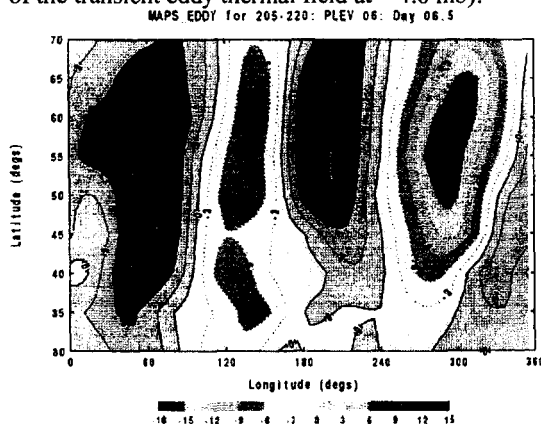
middle of southern winter during the first mapping year. These intervals allow an excellent comparison of the eddies in the north and south, as well as an initial look at the variation of the eddies with season in each hemisphere.

Results:

We summarize some of the basic results of the analyses below, separately for each seasonal interval.

Early northern winter This interval covers the range of $L_s \sim 205-220$ in the first mapping year, a period in early winter before the occurrence of a major regional dust storm - the Noachis Terra storm. Fairly strong eddy activity is present in northern middle/high latitudes during this period - one in which the mean thermal gradients are not as sharp as they are later on in the winter - as eddy temperature variance values are $\sim 40-60 \text{ K}^2$ at both lower and upper levels.

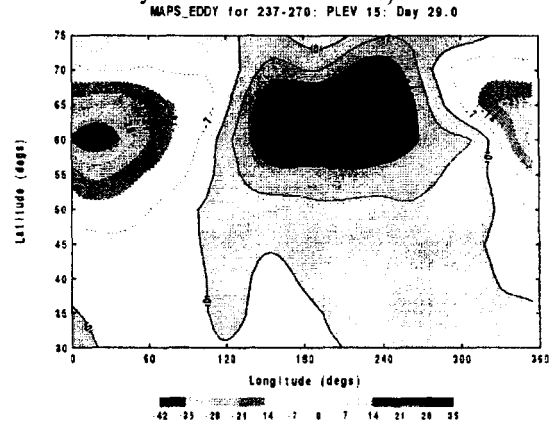
The largest amplitude transient eddy mode in this seasonal interval has a period of $\sim 5-10$ sols. Zonal wavenumber one has the largest amplitude, but wave 2 also has substantial amplitude. The wave 1 mode exhibits larger amplitudes at upper levels than at low ones; the wave 2 amplitudes are similar at lower and upper levels. The second dominant mode has a period of $\sim 2-4$ sols, and sizeable amplitudes at both wavenumbers 2 and 3. At wavenumber 2 there is significant amplitude at upper levels, though the largest amplitudes are at the lowest levels, while wave 3 is shallower. There is also a shorter period mode, with a period of $\sim 1.4-1.7$ sols, which has sizeable amplitudes at both wavenumbers 2 and 3. At times during the interval the eddy thermal field at low levels has a very regular and coherent structure around the planet (Fig. 1 below, showing an example of the transient eddy thermal field at $\sim 4.8 \text{ mb}$).



Stationary eddies are present, with substantial amplitude at both wavenumbers 1 and 2; wave 2 is the more dominant. The eddy activity is enhanced in storm zones, maximizing in the vicinity of Acidalia and Arcada.

Northern winter solstice I This interval covers the range of $L_s \sim 237-270$ in the first year, a period just following the Noachis Terra dust storm event. Eddy temperature variances are as large as $\sim 45 \text{ K}^2$ at lower levels and $\sim 225 \text{ K}^2$ at upper levels in northern middle and high latitudes. Thus, the eddies have a very strong upper-level character in this period.

Most prominent during this interval is an eastward-traveling, very large amplitude, zonal wavenumber one disturbance having a period of 15-25 sols (Fig. 2 below, showing an example of the transient eddy thermal field at 0.5 mb).



This disturbance has only small temperature amplitudes at low levels, so it is clearly not a typical baroclinically unstable mode. It appears to have a phase structure consistent with barotropic energy conversions, as well as baroclinic conversions. Such a slowly moving wave one mode has been found in GCM simulations. The large amplitudes of this mode during the period just after the dust storm event certainly suggest that it is favored by a more intense zonal-mean circulation. There have been recent speculations that it could be associated with inertial instabilities in low latitudes (7).

A number of other transient eddy modes are also present in this interval. One mode is also primarily zonal wavenumber one, but its period is $\sim 6-8$ sols. It exhibits large amplitudes at upper levels, but also has (relatively) much larger amplitudes at low levels than the 15-25 sol mode. A wavenumber one mode with a period of $\sim 6-8$ sols is prominent in the Viking data, as well as in GCM simulations (1,2,3). The GCM studies indicate that this mode is a typical baroclinic one associated with the surface temperature gradient, whose low level temperature maximum cannot be seen by TES. The other prominent mode during this interval is a wavenumber two disturbance with a period of 3-4 sols. It has maximum temperature variance at the lowest levels, but also exhibits a secondary maximum at upper levels.

A very pronounced storm track structure characterizes the transient eddy activity in this period, with the largest variances (more than double the smallest

values) occurring in the vicinities of Acidalia and Arcada. The storm tracks persist to the highest levels. Large amplitude stationary wavenumber one and two eddies are present in this period, with wave 2 dominating at lower levels.

Northern winter solstice II This interval covers the range of $L_s \sim 270-293$ during the first year; by this time the effects of the Noachis Terra storm had disappeared. Strong transient eddy activity is present, with variances as large as $\sim 45 \text{ K}^2$ at low levels and $\sim 125-150 \text{ K}^2$ at upper levels. The eddies thus do not have as much of an upper-level structure as those present before the solstice, and this is largely due to a considerable reduction in the amplitude of the long-period wave one mode. The sharpness of the mean thermal gradients is reduced in this interval, but not very greatly compared to the period prior to the solstice.

The variance due to the slow wave one mode is roughly a factor of three smaller than in the interval prior to the solstice. The relatively fast wave one mode ($\sim 6-8$ sols) variance, however, is increased by a factor of about three. The 6-8 sol mode also has a strong wavenumber 2 component. The dominant wave 2 mode has a period of ~ 3.5 sols, with maximum amplitudes at the lowest levels. There is also a mode with a period of 2-2.5 sols, at both wavenumbers two and three, which is very shallow.

The transient eddy activity is characterized by pronounced storm zones as in the period before solstice, and the location of these is very similar. Large amplitude stationary wave one and two eddies are again present, with wavenumber two being larger at both lower and upper levels.

Northern spring equinox This interval spans $L_s \sim 350-10$ in the first year, a period during which the VL-2 meteorology data show very strong transient eddy activity in midlatitudes (1). The examination of this interval has been hindered by relatively poor TES data coverage, as we have not been able to perform a full FFSM analysis poleward of 60 N. The temperature variance due to the transient eddies increases towards the pole, and there are values as large as $\sim 30 \text{ K}^2$ at 60N at low levels, with the upper level values not exceeding $\sim 25 \text{ K}^2$ at 60 N. The eddies are thus much shallower than they are earlier in the winter season.

The bulk of the transient eddy activity in this period is associated with a mode having a period of $\sim 2.5-3.5$ sols. This mode has sizeable amplitudes at both wavenumbers 2 and 3. At wavenumber 1 there is a mode with a period of 5-10 sols.

Enhanced eddy activity is found in the vicinity of Acidalia and Arcada, much as is the case near winter solstice. The amplitudes of the stationary eddies, waves 1 and 2, are much reduced compared to the

two solstice periods, and these eddies have a shallower vertical structure than those present in the winter season.

Southern winter solstice I: This interval covers $L_s \sim 75-90$ in the second mapping year, a period for which GCM simulations exhibit very weak transient eddy activity. The analysis of the TES data confirms that the transient eddy activity is indeed very weak near southern winter solstice. The eddy temperature variance does not exceed 15 K^2 and 25^2 at low and high levels, respectively - and typical values are substantially smaller than this.

A wavenumber one mode with a period of $\sim 6-8$ sols is present, having a very similar structure to the analogous mode in northern winter. There is also a westward propagating disturbance present with a period of roughly 2 sols, which has an upper-level amplitude maximum.

The weak eddy activity is concentrated in a region roughly centered on Argyre. A very large amplitude wave one stationary eddy is present, as well as a weaker wave 2 eddy.

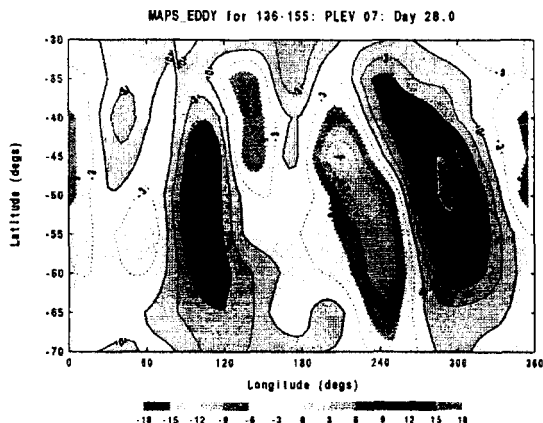
Southern winter solstice II This interval spans $L_s \sim 93-111$ in the second mapping year, also a period for which GCM's exhibit very weak transient eddy activity. The FFSM analysis also yields quite weak eddies, with maximum low-level variance values of $\sim 15-20 \text{ K}^2$ and average values much smaller than that; upper level variances do not exceed $\sim 30-35 \text{ K}^2$ with much smaller average values.

A wave one disturbance with a period of $\sim 8-10$ sols is present, along with a westward propagating wave one mode with a period of ~ 1.2 sols. The strongest transient eddy is a wavenumber three mode with a period of about 3.5 sols. This mode has a very shallow vertical structure.

The transient eddy activity is strongest again at lower levels in a region roughly centered on Argyre. A stationary wave one eddy is present at large amplitude, along with a weaker wavenumber two eddy.

Mid-southern winter This interval covers $L_s \sim 136-155$ during the first mapping year. Analyses of MGS RS data for this time period show relatively strong transient eddy activity, as do at least some GCM simulations. The FFSM analysis for this period yields transient eddy variances at low levels which are as large as $\sim 90 \text{ K}^2$, with upper-level values as large as $\sim 30 \text{ K}^2$. These mid-winter eddies in the south are thus quite shallow in the vertical.

The bulk of the transient eddy activity during this period is associated with a mode having a period of $\sim 2.2-2.5$ sols (Fig. 3 below, showing an example of the transient eddy thermal field at ~ 3.7 mb).



This is the same disturbance that has been found in RS data for this season (8). This mode has significant amplitudes at zonal wavenumbers 1-4, with waves 2 and 4 being the largest. The structure of this mode is very shallow, with maximum amplitudes located at the lowest levels at all wavenumbers, in the vicinity of 55 S.

The existence of substantial amplitudes at wavenumbers 1-4 implies a strong storm track structure during this season in the south. The eddy activity is strongest between 180 and 360 E, with the most vigorous activity again located in the vicinity of Argyre. Large amplitude stationary wave one and two disturbances are present in this seasonal interval; the wavenumber 2 eddy has a very shallow structure.

Discussion:

FFSM analysis has been performed on seven different seasonal intervals of TES nadir temperature data, including winter solstice periods in both hemispheres. The results of the analysis confirm the GCM-based prediction of very weak transient eddy activity near winter solstice in the south (1). The northern winter solstice eddies in the first mapping year (following a regional dust storm event) exhibit very large upper-level amplitudes. Prior to winter solstice, a ~ 15 -25 sol, wavenumber one disturbance is very prominent at upper levels. Following solstice this disturbance is still present, but a ~ 6 -8 sol, wave one mode dominates (this mode being present prior to solstice as well). Earlier in the first year winter, before the dust storm, the transient eddy activity is marked by substantial amplitudes at wavenumbers 1-3. A version of the wave one, 6-8 sol mode is present, along with ~ 2 -4 sol and ~ 1.4 -1.7 sol modes at both wavenumbers 2 and 3. The early winter eddies have maximum amplitudes substantially further poleward at low levels than those near solstice. This appears to be a consequence of the structure of the mean thermal field – the strongest meridional temperature gradients are located further equatorward near solstice. Fairly strong transient eddy activity exists near spring equinox in the north, but these

eddies have much shallower structures than those during the winter season.

The mid-winter season in the south (Ls ~ 136 -155) is a very interesting one, in that the low-level eddy activity is quite strong. These eddies are very shallow in nature, which appears to directly reflect the shallowness of the meridional temperature gradients in the zonal-mean flow at this season.

In all the intervals that have been examined to date, the transient eddy activity is very substantially enhanced in certain longitudinal regions. There are strong storm zones, as predicted on the basis of GCM simulations (9). In the north, the storm zones are located in the Acidalia and Arcada regions, which are broad lowlands. In the south, the eddy activity appears to be strongest in a region centered roughly on the Argyre basin. In all cases, the storm zones appear to correlate with trough regions in the zonal flow.

The structure of the transient eddies varies greatly with season and hemisphere. In particular, the eddies in northern winter are extremely deep, with very large amplitudes at upper levels. In early northern winter the eddies are much shallower, and they are shallower yet near spring equinox. In the south, the eddies are relatively shallow in all three of the intervals examined to date. The zonal flow is strongest and the upper level meridional temperature gradients are sharpest near northern winter solstice (in the first mapping year), and such a basic state appears to yield very deep eddies. GCM studies have shown a similar behavior (1).

Along with weak transient eddies near southern winter solstice, GCM simulations have evidenced very large amplitude stationary wave one amplitudes in southern winter. The TES data confirm this basic picture of the southern winter solstice planetary eddies. Near northern winter solstice, the TES data reveal large amplitude transient eddies, as well as fairly large amplitude stationary eddies. GCM studies have found a similar basic picture of the planetary eddies in the two winter hemispheres (1,10).

The observed mid-winter transient eddies in the south are much more vigorous than those near solstice, and preliminary examinations of the TES data appear to show even stronger eddy activity near the southern fall and spring equinox seasons. All of this activity appears to be largely confined to very low levels.

In summary, FFSM analysis of TES nadir temperature data has yielded a basic determination of the planetary eddy properties and structures during seven different seasonal intervals in both hemispheres. The results confirm the basic GCM-based picture of strong northern and weak southern transient eddies during the solstice seasons. Relatively strong eddy activity is present during the middle of southern winter, though it is confined to low levels. Fairly strong

activity is present in the north in early winter as well as near spring equinox, though these eddies are much shallower than the very deep ones which are present in the winter solstice season. Storm zones are very prominent in all of the seasonal intervals examined to date.

References:

- (1) Barnes, J.R., J.B. Pollack, R.M. Haberle, R.W. Zurek, C.B. Leovy, H. Lee, and J. Schaefer, 1993, *J. Geophys. Res.*, **98**, 3125-3148.
- (2) Barnes, J.R., 1980, *J. Atmos. Sci.*, **37**, 2002-2015.
- (3) Barnes, J.R., 1981, *J. Atmos. Sci.*, **38**, 225-234.
- (4) Banfield, D., B.J. Conrath, M.D. Smith, P.R. Christensen, and R.J. Wilson, 2002, *Icarus*, in press.
- (5) Salby, M.L., 1982, *J. Atmos. Sci.*, **39**, 2577-2600.
- (6) Salby, M.L., 1982, *J. Atmos. Sci.*, **39**, 2601-2614.
- (7) Wilson, R.J., D. Banfield, B.J. Conrath, and M.D. Smith, 2002, *Geophys. Lett.*, in press.
- (8) Hinson, D. P., and R.J. Wilson, 2002, *Geophys. Res. Lett.*, in press.
- (9) Hollingsworth, J.L., R.M. Haberle, J.R. Barnes, A.F.C. Bridger, J.B. Pollack, H. Lee, and J. Schaefer, 1996, *Nature*, **380**, 413-416.
- (10) Barnes, J.R., R.M. Haberle, J.B. Pollack, H. Lee, and J. Schaefer, 1996, *J. Geophys. Res.*, **101**, 12,753-12,776.

Introduction:

The Martian atmosphere is a highly dynamic environment, characterized by major changes on a daily basis. Transient baroclinic eddies contribute greatly to this variability – the weather – as do thermal tides, and smaller-scale circulations. The MGS TES atmospheric temperature data now permit the daily variability of Martian weather to be seen, globally, for the first time. Fast Fourier Synoptic Mapping (FFSM) is an analysis method that allows synoptic maps to be constructed from the highly asynchronous TES data. FFSM preserves the full space-time resolution of the data, without distorting or smoothing higher frequency phenomena such as weather systems. During periods when both ascending and descending (2 PM and 2 AM) orbital data is available, the frequency resolution of the TES data is equivalent to two synoptic maps per sol. During periods for which either ascending or descending data are available, but not both, the resolution is only one map per sol. In any case, FFSM readily allows the generation of maps at arbitrary frequencies and times.

A considerable amount of mapping orbit, nadir, TES temperature data have been subjected to FFSM analysis. A wide range of seasonal periods have been analyzed, from more than two full Mars years. The basic product is synoptic temperature maps. From these maps, the geopotential height field can be estimated, along with the horizontal winds. The combination of these products constitute Mars weather maps, which allow the very dynamic nature of the atmosphere to be depicted.

Data Analyses:

MGS TES nadir temperature data have been binned into one-degree wide latitude bins, spaced at 5 degree intervals. Maps have been produced for a number of the TES pressure levels, ranging from the lowest scale height to 30-40 km above the surface. Typically, intervals of data of about 20-40 sols in length are subjected to the FFSM analyses. Space-time spectra are a by-product of the analyses, and these are extremely useful for detailed studies of the circulation. The maps are produced at one-half sol intervals, nominally. For periods with insufficient data, the nominal interval is one sol. For animation or other purposes, the maps are often generated at much shorter time intervals. Several different basic

types of maps have been produced. These include maps showing only the transient eddy (non-tidal) portion of the temperature field, and the total (non-tidal) temperature field. Maps including the westward diurnal tide can be produced, but this tide is not fully resolved by TES.

Using the results from the FFSM analyses of temperatures, maps of the geopotential heights can be constructed. At present, these maps are based upon an assumption of a flat geopotential surface at some pressure level near the ground (this is equivalent to assuming zero horizontal winds at this level). Using the geopotential maps, synoptic maps of the horizontal winds can then be produced. A linear balance approach has been used to determine the winds. This approach yields much better wind estimates than geostrophic or gradient wind balance does, when the winds are fairly strong. It also offers some major advantages when combined with the FFSM method. Weather maps combining the height data, the temperature data, and the wind data, are then constructed.

Results:

In the fall, winter, and spring seasons, the synoptic maps evidence a highly dynamic atmosphere. In the summer season, the atmosphere is much less dynamic except at high latitudes (except for the tides). Weather systems grow and decay on short time scales (as short as one sol or less), and can move rapidly both zonally and meridionally. Front-like structures are often prominent. In both hemispheres the weather systems preferentially amplify in certain regions – storm zones (Figs. 1 and 2). At times, the systems have a highly global structure. The systems are of planetary scale, being dominated by zonal wavenumbers 1-3. The larger scale systems have extremely deep structures, with large amplitudes at very high levels. An extreme example of this is a very-large amplitude disturbance which is present during northern winter (Fig. 3). It is dominated by wavenumber one, and has only small amplitudes near the ground. It propagates to the east quite slowly (having a period of ~ 15-25 sols), but this propagation is actually rather complex when viewed in the maps. This disturbance is almost certainly not the same basic kind of weather system as the others in the maps, and it may have no real terrestrial counterpart. It does appear to be quite characteristic of the Martian northern winter atmosphere under dusty conditions.

Near to the winter solstice season, the weather systems in the northern hemisphere are much stronger than those in the south (Figs. 4 and 5). This is basically in agreement with the results of GCM simulations, and appears to be a result of both the topography of Mars and the eccentricity of the orbit. However, later in southern winter the systems are found to be much more vigorous. They are also more vigorous in early spring in the south. The southern hemisphere weather systems are somewhat different than those in the north, as they are largely confined to the western hemisphere and especially to the vicinity of the southern extension of Tharsis and Argyre (Fig. 6). They tend to have relatively shallow vertical structures, and tend to be characterized by shorter zonal scales than the northern winter systems. They also have shorter dominant periodicities.

The northern weather systems are typically marked by strong storm zones. These storm zones basically coincide with the broad lowland regions in the north: Acidalia and Utopia/Arcadia. They can extend to very high altitudes. Especially within these regions, the weather systems are often seen to penetrate well to the south (Fig. 7). A similar behavior has been seen in the MOC imagery in late winter and spring, when it is associated with dust events. The weather systems near the winter solstice season in the north tend to have very deep structures, while those in the fall and in the spring are much less deep. The systems tend to be located further south in winter, and are located at higher latitudes in the early fall and the spring seasons. They always are located near the region in which the north-south temperature gradients are strongest, which tends to be near the edge of the seasonal polar cap.

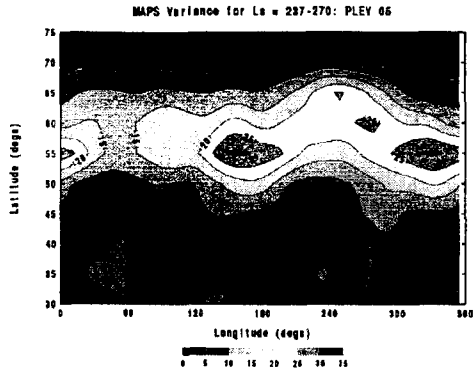
The very strong global dust storm which began in early fall in the second MGS mapping year had a strong impact on the weather systems. They were greatly diminished in strength in comparison with the systems in the same season in the first mapping year. This is consistent with observations made by the Viking Landers during the first Viking year. Later on, when this global storm was still raging, the slowly moving, wave-one disturbance was present in the north at very large amplitudes. There are considerable differences in the weather system activity in the two Mars years of MGS mapping, and the bulk of these appear to be associated with regional and global dust storm activity.

Summary:

FFSM analyses of MGS TES nadir temperature data have allowed the construction of Mars weather maps: synoptic maps showing temperatures, geopotential heights, and horizontal winds on constant pressure surfaces. The winds have been determined by making use of a linear balance approach, which is much more accurate than geostrophic balance when the winds are fairly strong. It is assumed that the winds vanish at a pressure level near the ground, in the absence of sufficiently accurate surface pressure data. Maps have been produced for a wide range of seasons in both hemispheres, at levels between the surface and ~ 40 km, for more than two full Mars years.

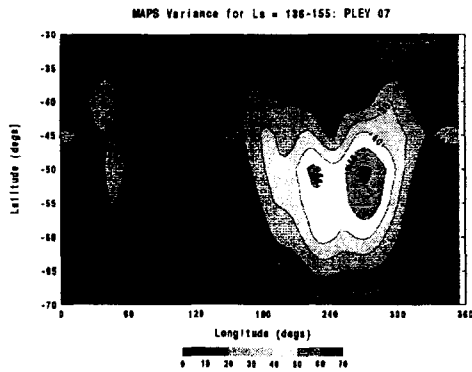
The maps show a highly dynamic atmosphere in the fall, winter, and spring seasons. Weather systems are seen to grow and decay on short time scales, and can move very rapidly. They tend to amplify in certain regions – storm zones – which are strongly correlated with the topography. The storm zones have very different structures in the two hemispheres, presumably reflecting the very different topography in the two hemispheres. The weather systems can have very deep vertical structures, with some of them exhibiting maximum amplitudes at very high levels (~ 30 - 40 km or above). Near to the winter solstice seasons, the northern weather systems are much stronger than their southern counterparts – much as predicted by GCM studies. The northern systems also tend to be of larger scale and to have deeper structures. They tend to have longer periodicities.

The weather maps allow the highly dynamical nature of the atmosphere to be clearly seen. This is limited by the difficulty that the TES retrievals have in sampling the lowest part of the atmosphere, and by the relatively coarse resolution of these retrievals. Nonetheless, a great deal of complex weather activity is apparent in the periods which have been mapped to date, and this activity differs substantially between the two MGS mapping years. The synoptic maps have considerable potential, in synergy with MOC imagery, and TES dust and water vapor/ice data, to give us a much better picture of the atmospheric part of the climate system of Mars. Such studies are currently underway.



APR Sun Nov 3 14:29:53 2003

Figure 1: Temperature variance of the weather systems in northern winter, at the 6.1 mb level.



APR Sun Nov 3 14:29:53 2003

Figure 2: Temperature variance of the weather systems in southern mid-winter, at the 3.7 mb level.

QuickTime™ and a Photo - JPEG decompressor are needed to see this picture.

Figure 3: A synoptic map of upper-level temperatures during a northern winter period when the slow, wavenumber one disturbance is dominant.

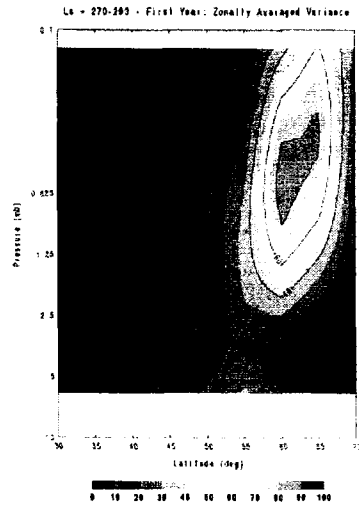


Figure 4: Zonally-averaged weather system temperature variance for a northern winter solstice period.

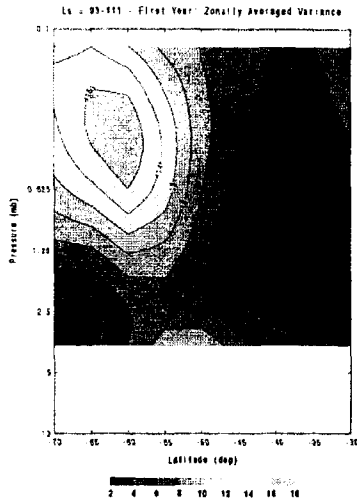


Figure 5: Zonally-averaged weather system temperature variance for a southern winter solstice period.

QuickTime™ and a Photo - JPEG decompressor are needed to see this picture.

Figure 7: A synoptic map of temperatures associated with northern weather systems during the first mapping year fall season.

QuickTime™ and a Photo - JPEG decompressor are needed to see this picture.

Figure 6: A synoptic map of temperatures associated with southern weather systems during mid-winter.

REPORT DOCUMENTATION PAGE			Form Approved OMB No. 0704-0188	
Public reporting burden for this collection of information is estimated to average 1 hour per response, including the time for reviewing instructions, searching existing data sources, gathering and maintaining the data needed, and completing and reviewing the collection of information. Send comments regarding this burden estimate or any other aspect of this collection of information, including suggestions for reducing this burden, to Washington Headquarters Services, Directorate for Information Operations and Reports, 1215 Jefferson Davis Highway, Suite 1204, Arlington, VA 22202-4302, and to the Office of Management and Budget, Paperwork Reduction Project (0704-0188), Washington, DC 20503.				
1. AGENCY USE ONLY (Leave blank)	2. REPORT DATE 12-29-03	3. REPORT TYPE AND DATES COVERED Final 7-01-00 to 6/30/03		
4. TITLE AND SUBTITLE Studies of MGS TES and MPF MET Data			5. FUNDING NUMBERS NAG 5-9771	
6. AUTHOR(S) Jeff R. Barnes				
7. PERFORMING ORGANIZATION NAME(S) AND ADDRESS(ES) Oregon State University Corvallis, OR			8. PERFORMING ORGANIZATION REPORT NUMBER NS109A	
9. SPONSORING/MONITORING AGENCY NAME(S) AND ADDRESS(ES) ONR			10. SPONSORING/MONITORING AGENCY REPORT NUMBER	
11. SUPPLEMENTARY NOTES				
12a. DISTRIBUTION/AVAILABILITY STATEMENT Unlimited Public Access			12b. DISTRIBUTION CODE	
13. ABSTRACT (Maximum 200 words) <p>The work supported by this grant was divided into two broad areas:</p> <p>(1) mesoscale modeling of atmospheric circulations and analyses of Pathfinder, Viking, and other Mars data, and (2) analyses of MGS TES temperature data.</p> <p>The mesoscale modeling began with the development of a suitable Mars mesoscale model based upon the terrestrial MM5 model, which was then applied to the simulation of the meteorological observations at the Pathfinder and Viking Lander 1 sites during northern summer. This extended study served a dual purpose: to validate the new mesoscale model with the best of the available in-situ data, and to use the model to aid in the interpretation of the surface meteorological data.</p>				
14. SUBJECT TERMS			15. NUMBER OF PAGES	
			16. PRICE CODE	
17. SECURITY CLASSIFICATION OF REPORT	18. SECURITY CLASSIFICATION OF THIS PAGE	19. SECURITY CLASSIFICATION OF ABSTRACT	20. LIMITATION OF ABSTRACT	